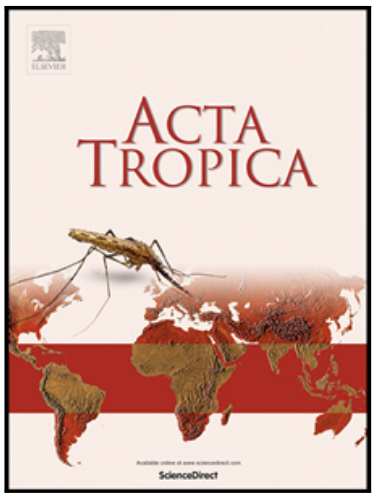

Metabolome alterations in Clonorchis sinensis after treatment with tribendimidine and praziquante in vivo

Wei Yufen , Liu Xinru , Xue Jian , Huolele , Jiang Zhihua , Chen Yu , Liang Mingyong , Zhang Haobing

PII: S0001-706X(22)00029-8
DOI: https://doi.org/10.1016/j.actatropica.2022.106330
Reference: ACTROP 106330

To appear in: *Acta Tropica*

Received date: 15 July 2021
Revised date: 19 January 2022
Accepted date: 23 January 2022

Please cite this article as: Wei Yufen , Liu Xinru , Xue Jian , Huolele , Jiang Zhihua , Chen Yu , Liang Mingyong , Zhang Haobing , Metabolome alterations in Clonorchis sinensis after treatment with tribendimidine and praziquante in vivo, *Acta Tropica* (2022), doi: https://doi.org/10.1016/j.actatropica.2022.106330

Metabolome alterations in *Clonorchis sinensis* after treatment with tribendimidine and praziquante in vivo

Wei Yufen[a1], Liu Xinru[b1], Xue Jian[a], Huolele[a], Jiang Zhihua[c], Chen Yu[d], Liang Mingyong[d], Zhang Haobing[a*]

[a] National Institute of Parasitic Diseases, Chinese Center for Disease Control and Prevention; NHC Key Laboratory of Parasite and Vector Biology (National Institute of Parasitic Diseases, Chinese Center for Disease Control and Prevention), Shanghai 200025, China

[b] Translational Medical Institute, Shanghai University, Shanghai 200444, China

[c]Guangxi Zhuang Autonomous Region Center for Disease Control and Prevention, Nanning 530028, China

[d] Heng County Center for Disease Control and Prevention, Heng County 530300, China

[1] Contributed equally to the article

* Corresponding author, E-mail address: zhanghb@nipd.chinacdc.cn

Corresponding author at: 207 Rui Jin Er Road, Shanghai 200025, People's Republic of China.

Supported by the Fifth Round of Three-Year Public Health Action Plan of Shanghai (No. GWV-10.1-XK13).

Highlights

- The metabolomes of *C. sinensis* in rats after TBD /PZQ administration were measured.
- TBD administration caused an alteration in amino acids and lysophospholipids.
- The membrane may destroyed by lysophospholipids, which lead to *C. sinensis* death.

Abstract: Tribendimidine (TBD) is a broad-spectrum anthelmintic drug that is also significantly effective in treating clonorchiasis. In this study, the altered metabolomes of *Clonorchis sinensis* (*C. sinensis*) in rats after TBD administration were quantified by using ultrahigh-performance liquid chromatography-tandem mass spectrometry (*UHPLC–MS/MS)* and gas chromatography-mass spectrometry (*GC–MS*) to explore the possible active sites of TBD against clonorchiasis through altered metabolites and metabolic pathway analysis, and the results are expected to provide a target for the future design of anti-*Clonorchis sinensis* drugs. The worm burden reduction rate and scanning electron microscopy demonstrated that

praziquantel (PZQ, positive control drug) and TBD had significant effects on *C. sinensis* in rats after treatment at a single dose of 200 mg/kg for 24 h. For the MS-based metabolomic analysis, a total of 173 standard metabolites (126 amino acids, 10 phospholipids and 37 fatty acids) were utilized as a reference metabolite database for metabolome identification. In total, 32 amino acids, 71 phospholipids and 27 fatty acids were detected in the *C. sinensis* of each group. Among these metabolites, 10 amino acids were significantly decreased in both drug-treated groups. Four lysophosphatidyl cholines (LPCs), six lysophosphatidyl ethanolamines (LPEs) and one phosphatidyl inositol (PI) were significantly increased after treatment with TBD. There were no significant changes in fatty acids among the control group and the two drug-treated groups. The results indicated that TBD administration caused a decrease in amino acids involved in the metabolic pathways of energy consumption and an increase in lysophospholipids, which are the hydrolysis products of phospholipase2 (PLA2) in the phospholipid metabolic pathways. The increased lysophospholipid content can destroy the cell membrane, increase membrane permeability, and even cause exposure to internal antigens that can be attacked by host antibodies. Perhaps the destroyed membrane, the exposed internal antigens and the consumed energy are the cause of the damage and death of *C. sinensis* after TBD administration. This is an interesting problem that can be examined in future research.

Key words: Metabolome alterations; Tribendimidine; Praziquante; *Clonorchis sinensis*; Amino acids; Phospholipids; Fatty acids

1. Introduction

More than 35 million people are infected with the liver fluke *Clonorchis sinensis* (*C. sinensis*) worldwide (Prociv, 1995). Among them, approximately 15 million infected people live in China, the Republic of Korea, northern Vietnam and part of Russia (Jennifer and Jürg, 2005; Lun et al., 2005). *C. sinensis* infection causes pathological changes in the bile duct, liver, and gallbladder. Individuals with heavy infections often suffer from unspecific symptoms, such as fever, fatigue, weakness, nausea, and/or abdominal pain, but more severe consequences, namely, obstructive jaundice and biliary colic, can occur, and the most serious consequences of clonorchiasis are cholangiocarcinoma and bile duct cancer (Vennervald and Polman, 2010; Furst et al., 2012; Hong and Fang, 2012). Praziquantel (PZQ) and albendazole are the most common chemotherapeutic compounds against human clinical clonorchiasis, and they have been used for nearly 40 years (Löscher et al., 1982; Yangco et al., 1987), usually at doses of 70 mg/kg t.i.d. for 3 consecutive days and 10 mg/kg b.i.d. for 7 consecutive days in clinic (Yangco et al., 1987; Liu et al., 1991). However, large doses of these compounds can lead to significant side effects, and patients often reduce the dosage by themselves, which leads to a decrease in efficacy. In addition, resistance to PZQ and albendazole has been reported in several

papers (Coles et al., 2000; Botros and Bennett, 2007; Doenhoff et al., 2008a). Thus, it is necessary to find new anti-*Clonorchis sinensis* drugs.

Tribendimidine (TBD) is a broad-spectrum anthelmintic drug that was synthesized by the National Institute of Parasitic Diseases, Chinese Center for Disease Control and Prevention in the mid-1980s (Ren et al., 1987). It works well against *N. americanus, Nippostrongylus braziliensis, Syphacta mesocriceti, Ancylostoma caninum, Toxocara canis, Amoebotaenia cuneata,* and *Davainea proglottina* (Xiao et al., 2005). In particular, the effect of TBD against *N. americanus* infection at a single oral dose was superior to that of albendazole under the same single dose, and because it has fewer adverse effects, TBD was approved by the Chinese State Food and Drug Administration in 2004 as an antihelmintic drug (Xiao et al., 2005). In recent years, through experimental studies and clinical observation, TBD was observed to be highly effective in treating clonorchiasis (Keiser et al., 2007; Xiao et al., 2009a; Boughton et al., 2011). With a single dose of 150 mg/kg, the worm burden reductions of TBD and PZQ were 89.5% and 80.7%, respectively, after treatment for 2 weeks in rats infected with adult *C. sinensis*. Even with a single dose of 75 mg/kg, the worm burden of TBD was still 71.4%, but that of PZQ was only 20.7% (Xiao et al., 2008). The results of clinical trials also showed that the treatment efficacy of TBD was better than that of PZQ in Chinese patients with clonorchiasis and had fewer adverse events than PZQ (Qian et al., 2012). However, the TBD cure rate did not reach 100% after increasing the dosage (Xiao et

al., 2009a). As a potential drug candidate for treating clonorchiasis, the mechanism of TBD in the treatment of clonorchiasis is not yet clear. What substances changed in the worm body after TBD application? How do changes occur? Can we identify drug targets of TBD that can provide new drug design clues? Furthermore, exploring endogenous metabolite alterations in *C. sinensis* after treatment with TBD is a good strategy for answering these questions and may provide clues about TBD drug targets in *C. sinensis* and help design new drugs on the basis of the targets.

In this study, quantified metabolomic methodologies were applied to investigate altered metabolic changes in *C. sinensis* after treatment with TBD and PZQ. Metabolomic technology is a powerful holistic analytical approach that is widely applied in studies of disease pathogenesis (Zhao et al., 2010; Lal and Ambalavanan, 2015; Qiang, 2016), drug toxicity (Nicholson, 2003; Keun, 2006) and nutritional sciences (Claus and Swann, 2013). It has also been applied in parasitological studies with comprehensive characterizations of the host metabolic responses to infections by several parasites, such as *Trypanosoma brucei brucei* (Wang et al., 2008), *Plasmodium berghei* (Ghosh et al., 2012; Sonawat and Sharma, 2012) and *Echinostoma caproni* (Ciara et al., 2013). In this study, the major metabolites in the homogenates of *C. sinensis*, such as amino acids and phospholipid acids, were determined by ultra-performance liquid chromatography tandem mass spectrometry (*UHPLC–MS/MS*), and fatty acids were measured by gas chromatography–mass

spectrometry (*GC–MS*) to observe the changes in these metabolites in *C. sinensis* collected from 24 h TBD- or PZQ-treated rats.

2. Materials and Methods

2.1 Drugs, reagents and materials.

TBD was provided by the Shandong Xinhua Pharmaceutical Company Limited (Zibo, PR China). PZQ was purchased from the Shanghai No. 6 Pharmaceutical Company (Shanghai, China). Tween 80, ethanol and 0.9% normal saline were purchased from Aladdin Biochemical. Ultra-pure water was prepared with a Milli-Q water purification system (Millipore, MA, USA). Formic acid, hexane, methanol, ammonium acetate and acetonitrile (HPLC grade) were purchased from Thermo Fisher (Thermo Fisher Scientific Inc., USA). $K_2HPO_4 \cdot 3H_2O$ and $NaH_2PO_4 \cdot 2H_2O$ (AR grade) were purchased from the SCRC (Sinopharm Chemical Reagent Co., Ltd., China). AR grade N-ethylmaleimide (NEM), boric acid, dimethylsulfoxide (DMSO), 4-tert-butylbenzenethiol (tBBT), 5-aminoisoquinoline (5-AIQ), ascorbic acid, N,N'-disuccinimidyl carbonate (DSC), ethylenediaminetetraacetic acid (EDTA) and phosphinehydrochloride (TCEP) were purchased from Sigma–Aldrich (Sigma–Aldrich, Inc., USA). Chloroform (HPLC grade) was purchased from Duksan Pure Chemicals (Seoul, Korea). K_2CO_3 used for GC–MS detection (analytical grade) was purchased from the SCRC (Sinopharm Chemical Reagent Co., Ltd., China). A total of 126 amino analyte standards were purchased from Sigma–Aldrich (Sigma–Aldrich, Inc., USA) and J&K (J&K Scientific, China). Ten phospholipid internal

standards (ISs), PC (17:0/14:1), PE (17:0/14:1), PG (17:0/14:1), PS (17:0/14:1), PA (17:0/14:1), PI (17:0/14:1), LPC (17:1), LPE (17:1), LPA (17:1), and SM (d18:1/17:0), were purchased from Avanti Polar Lipids (Alabaster, AL, USA). Thirty-seven fatty acid methyl ester mixtures, heptadecanoic acid (C17:0), 2,6-di-*tert*-butyl-4-methylphenol (BHT), and acetyl chloride (analytical grade), were purchased from Sigma–Aldrich (Sigma–Aldrich, Inc., USA).

2.2 Rats.

A total of 68 male Sprague–Dawley (SD) rats weighing between 70 g and 80 g were purchased from the Shanghai Jihui Experimental Animal Feeding Co., Ltd. (Shanghai, China). Male rats were used because of the stable hormone level. Rats were kept at the SPF grade animal facility of the National Institute of Parasitic Diseases, Chinese Center for Disease Control and Prevention (Shanghai, China). The protocol for sampling animals was approved by the Animal Welfare & Ethics Committee of the National Institute of Parasitic Diseases, Chinese Center for Disease Control and Prevention in Shanghai (Permit No: IPD-2020-12).

2.3 The host-parasite model.

C. sinensis metacercariae were collected from freshwater fish (*Pseudorasbora parva*) caught from ponds in a clonorchiasis-endemic area of Heng County, Guangxi Province, China. The method was described previously (Xiao et al., 2008; Xiao et al., 2009b). In brief, after being crushed by a grinder, the fish were digested with a 1% pepsin-HCl solution for approximately 6 hours at 37 °C. Then, the supernatant was

removed, and the precipitates were washed several times with normal saline. Metacercariae were identified under a stereomicroscope, placed in a 1.5 ml ep tube and stored at 4 °C before infection. Sixty-eight SD rats were infected orally with 80 *C. sinensis* metacercariae. Five weeks postinfection, rats were treated with TBD or PZQ (suspended in 7% Tween 80 and 3% ethanol) orally at a single dose of 200 mg/kg, with twenty-five rats in each drug-treated group. Eighteen rats were untreated and served as controls. Twenty-four hours posttreatment, rats were euthanized by CO_2, all flukes were removed from the liver and bile ducts, and the number of flukes of each rat was recorded at the same time. After rinsing three times with cold HBSS, 7 flukes of each group were fixed in 2.5% glutaraldehyde phosphate buffer. Twenty flukes were collected as one sample and stored in liquid nitrogen as soon as possible for MS or GS detection. Seven samples were collected in each group.

2.4 Scanning electron microscopy.

The fixed *C. sinensis* of each group was dehydrated in a graded series of ethanol and acetone, dried with CO_2, coated with gold, and then examined with a Joel JSM-820 scanning electron microscope (Keiser and Vargas, 2010).

2.5 Sample preparation, UHPLC–MS/MS and GC–MS conditions.

2.5.1 Sample preparation and UHPLC–MS/MS conditions for the assay of amino acids.

C. sinensis (50 mg) was extracted with 500 μL of precooled methanol using TissueLyser at 50 Hz for 90 s, and then an aliquot (10 μL) was vortex-mixed with 80 μL of NEM solution (2.5 mM) in phosphate buffer (0.1 M, pH of 7.0) containing 10 mM ascorbic acid, 10 mM EDTA and 7% DMSO for 1 min. Ten microlitres of tBBT solution (1 M in DMSO) was added, followed by the addition of 700 μL of borate buffer (0.2 M, pH of 8.8) containing 20 mM TCEP and 1 mM ascorbic acid. After vortexing and settling for 2 min, 200 μL of a 5-AIQC solution was then added and incubated at 55 °C for 10 min. The mixture was cooled to ambient temperature, 2 μL of formic acid was added, and the solution was filtered through a 0.22 μm membrane filter before UPLC–MS/MS analysis.

UPLC–MS/MS consisted of an Agilent 1290 UPLC coupled to an Agilent 6460 triple quadrupole mass spectrometer equipped with an electrospray ionization (ESI) source (Agilent Technologies, USA). The 5-AIQC-tagged samples (1 μL) were individually injected onto a UPLC column (Agilent ZORBAX RRHD Eclipse XDB C18 column, 2.1 × 100 mm, 1.8 μm particles) with its temperature set to 50 °C. Water and methanol containing 0.1% (v/v) formic acid were used as two mobile phases A and B, with a flow rate of 0.5 mL/min. Electrospray ionization was performed in the positive ion mode. Multiple reaction monitoring (MRM) was used for quantification of screening fragment ions (Gu et al., 2007; Boughton et al., 2011).

2.5.2 Sample preparation and UHPLC–MS/MS conditions for the phospholipid assay.

Samples of 20 mg *C. sinensis* were extracted with 1000 μL of methanol-chloroform (1:1, v/v) using TissueLyser at 50 Hz for 90 s and mixed with 70 μL of the internal standard (10 μg/mL of each in methanol-chloroform (1:1, v/v)) and 450 μL of water. The tubes were briefly vortexed and then centrifuged (12000 rpm, 10 min, 4 °C), and the bottom layer was collected. This extraction process was repeated twice, and the combined bottom layers were evaporated to dryness and redissolved in 80 μL of methanol-chloroform (1:1, v/v) for UHPLC–MS/MS analysis. The treatment of the mixed sample (approximately 100 mg of tissues) for qualitative analysis was consistent with the sample preparation for quantitative analysis (Bligh and Dyer, 1959; Hsu and Turk, 2003; Kim et al., 2009).

The UHPLC–MS/MS instrument consisted of an Agilent 1290 UHPLC coupled to an Agilent 6460 triple quadrupole mass spectrometer equipped with an electrospray ionization (ESI) source (Agilent Technologies, USA). One microlitre of the extractwas injected onto a UPLC column (Agilent ZORBAX RRHD Eclipse XDB C18 column, 2.1 × 100 mm, 1.8 μm particles) with its temperature set to 50 °C. A binary isocratic elution with 98% B was applied, with water for solvent A and methanol for solvent B. Both solvents A and B included 0.01% formic acid and 5 mM ammonium acetate. The flow rate was 0.5 mL/min. The capillary voltage was set at 4.0 kV (positive ion mode) and 3.5 kV (negative ion mode).

2.5.3 Sample preparation and GC-FID/MS conditions for the fatty acid assay.

Samples (20 mg) were extracted with 500 μL of precooled methanol using a tissue lyser at 50 Hz for 90 s, and then an aliquot (100 μL) was mixed with 20 μL of the internal standard (1 mg/mL of C17:0, 2 mg/mL of BHT in hexane) and 1000 μL of methanol-hexane (4:1, v/v). The tubes were gently vortexed and then placed in a homemade liquid nitrogen bath for 10 min. Then, 100 μL of acetyl chloride was slowly added to the tubes and kept in the dark at room temperature for 24 h. Then, 2.5 ml of 6% K_2CO_3 solution was added slowly to stop the reaction and neutralize the mixture in an ice bath. After 200 μL of hexane was added to extract fatty acid methyl esters, the tubes were briefly vortexed and then centrifuged (3000 rpm, 10 min), and the top layer was collected. This extraction process was further repeated twice, and the combined top layers were evaporated to dryness and redissolved in 50 μL of hexane for GC analysis (Xu et al., 2010; An et al., 2013; Li et al., 2013).

Methylated fatty acids were measured on a Shimadzu GCMS-QP2010Plus spectrometer (Shimadzu Scientific Instruments, USA) equipped with a mass spectrometer with an electron impact (EI) ion source and a flame ionization detector (FID). An Agilent DB-225 capillary GC column (10 m, 0.1 mm ID, 0.1 μm film thickness) was employed with a sample injection volume of 1 μL and a splitter (1:60).

2.6 Data processing and analysis.

Peak determination and peak area integration were performed with MassHunter Workstation software (Agilent, Version B.06.00). Standard curves were constructed by least-squares linear regression analysis using the peak area ratio of derivatized individual standards against the nominal concentration of the calibrator. Quantification of samples was performed identically and then normalized by the dry weight of the samples. The SIMCA-P+ software package (V.12, Umetrics, Sweden) was employed for multivariate data analysis. Principal component analysis (PCA) was performed by using mean-centred NMR data to identify general trends and outliers. A supervised multivariate data analysis tool, orthogonal-projection to latent structure discriminant analysis (OPLS-DA), was employed with the Pareto scaling method (Wei et al., 2016). The significance was confirmed through one-way analyses of variance (ANOVAs) and Duncan's post-hoc tests using SPSS 14.0 software (SPSS Inc., Chicago, IL, USA). $P < 0.05$ was considered significant.

3. Results

3.1 The worm burden levels.

It has been reported that after one week of TBD treatment of *C. sinensis*-infected rats at a dose of 400 mg/kg, the worm burden reduction was approximately 95.7% (Keiser et al., 2007). However, the aim of this study was to collect enough worms for MS detection. In our pre-experiment, the worm burden was too low to collect enough flukes after treatment with TBD for 72 h or 48 h at a single dose of 300 mg/kg. Therefore, we collected the flukes after treatment for 24 h at a single dose of

200 mg/kg. The worm burden reduction rates were 28.45% and 77.33% after treatment with PZQ and TBD for 24 h, respectively, which demonstrated that TBD also had significant effects after treatment for 24 h.

Table 1. The worm burden of PZQ and TBD at a dose of 200 mg/kg

Group	Number of rats	Mean worm burden (SD)	% Total worm burden reduction
Control	18	35.0 (14.2)	-
Praziquantel	25	6.08 (3.6)	28.45
TBD	25	4.52 (2.9)	77.33

3.2 Scanning electron microscopy.

The drug effects on the tegument of *C. sinensis* are depicted in Figure 1. The ridges on the tegument of untreated worms were arranged in an orderly manner, and there were many small papillae on the ridges (Figure 1A). Twenty-four hours after 200 mg/kg of PZQ (Figure 1B) or TBD (Figure 1C) administration, the teguments were apparently damaged, the papillae disappeared, and most of the tegument exfoliated. These results also indicate the remarkable efficacy of PZQ and TBD on *C. sinensis* treated for 24 h at a dose of 200 mg/kg.

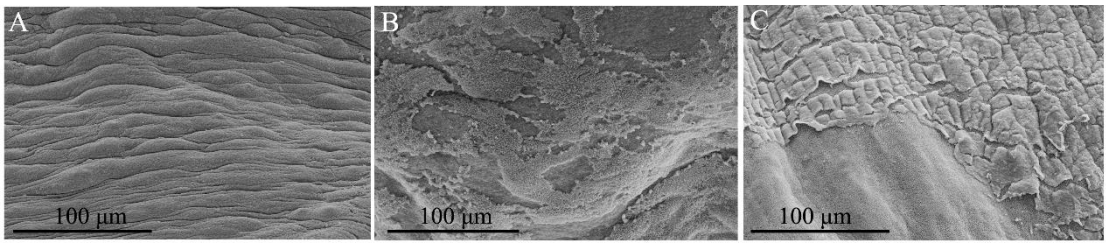

Figure 1. (A) SEM observations of adult *C. sinensis* recovered from normal rat bile ducts. (B) Tegument of *C. sinensis* recovered from rats after treatment with PZQ at a single dose of 200 mg/kg for 24 h. The tegument ridges collapsed, the tegument exfoliated, and the subtegmental tissues were exposed. (C) Tegument of *C. sinensis* recovered from rats after treatment with TBD at a single dose of 200 mg/kg for 24 h. The tegument was apparently damaged. The tegument sloughed, and subtegment tissues were exposed.

3.3 Amino acid metabolism.

A total of 120 commercial amino acid standards were used in this targeted detection. The results showed that 32 amino acid metabolites were detected in the worm homogenate samples, and nine amino acids changed significantly in the drug-treated group. Representative chromatograms of the metabolites are depicted in Figure 2. The peaks of the 9 significantly changed metabolites were numbered 1 to 9. The OPLS-DA score plots of the control, PZQ and TBD groups are depicted in Figure 3A. The three groups separated well in the score plot, which means they had significant changes from one another. All nine significantly changed amino acids were decreased in the TBD group compared with the control group (Table 2, Figure

4), and they were decreased more significantly in the TBD group than in the PZQ group. The results are consistent with the conclusion that TBD has a better anti-*C. sinensis* effect than PZQ (Jian et al., 2009). As shown in Figure 1, the tegument of *C. sinensis* was seriously damaged. After the drug is absorbed into the blood, it circulates to the hepatic portal vein and acts on the surface of the flukes, causing damage to the tegument, increasing the consumption of protein and amino acids, and generally reducing the content of amino acids. The more serious the damage is, the more the amino acid content decreases. At the same time, the depletion of amino acids also promoted the energy depletion of the worms and further led to worm death.

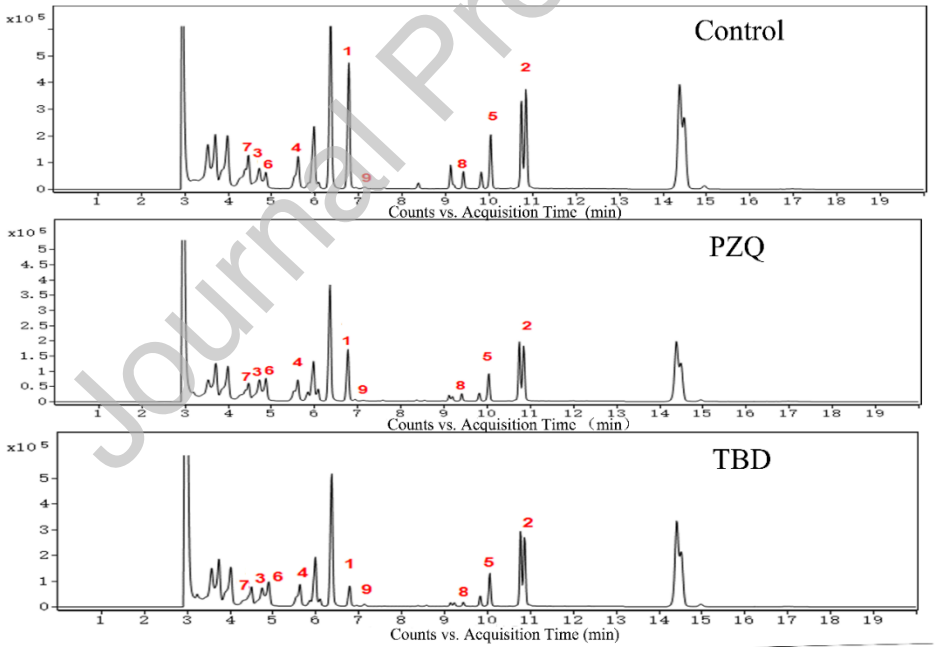

Figure 2. Representative chromatogram of amino acids in *C. sinensis*. The numbers are annotated as follows: 1. L-proline, 2. L-valine, 3. L-glutamine, 4. L-glutamic

acid, 5. L-methionine, 6. L-aspartic acid, 7. taurine, 8. L-ornithine, and 9. L-glutathione-oxidized.

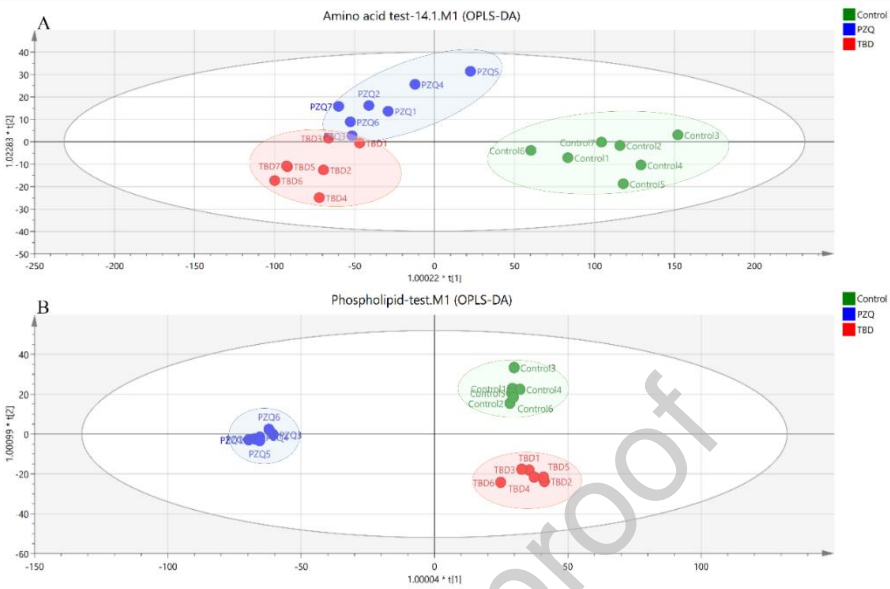

Figure 3. (A) OPLS-DA score plot of the control group, PZQ group and TBD group for amino acid detection. (B) OPLS-DA score plot of the control group, PZQ group and TBD group for phospholipid detection. (R2Y =0.98, R2X = 0.976, and Q2 = 0.703).

Table 2: Significant amino acids in *C. sinensis* after treatment with PZQ or TBD in rats in vivo.

Metabolites	Control (ng/mg)	PZQ (ng/mg)	TBD (ng/mg)	*p* (Con vs. PZQ)	*p* (Con vs. TBD)	Related pathway
L-Proline	2930.50±633.72	841.68±350.75	393.28±111.47	**	**	Arginine and proline metabolism
L-Valine	2727.74±639.00	2237.24±374.93	1926.04±307.39	-	*	Valine, leucine and isoleucine metabolism
L-Glutamine	3627.26±905.77	2637.08±388.52	2088.53±379.22	-	**	Glutamine metabolism
L-Glutamic acid	2632.21±701.98	2018.34±336.30	1451.56±359.26	-	*	Glutamic acid metabolism
L-Methionine	2527.79±631.65	1885.58±321.39	1578.08±250.23	-	**	Methionine metabolism
L-Aspartic acid	1398.28±285.54	1274.93±159.83	898.92±224.28	-	*	Aspartic acid metabolism
Taurine	977.38±278.45	707.11±136.36	491.29±140.26	-	**	Taurine and hypotaurine metabolism
L-Ornithine	368.18±75.16	169.06±128.84	81.05±30.28	**	**	Arginine and ornithine metabolism
L-Glutathione- oxidized	611.68±157.31	251.00±42.42	195.87±87.33	**	**	Glutamic acid, cysteine and glycine metabolism

-: $p>0.05$, *: $p<0.05$, **: $p<0.01$.

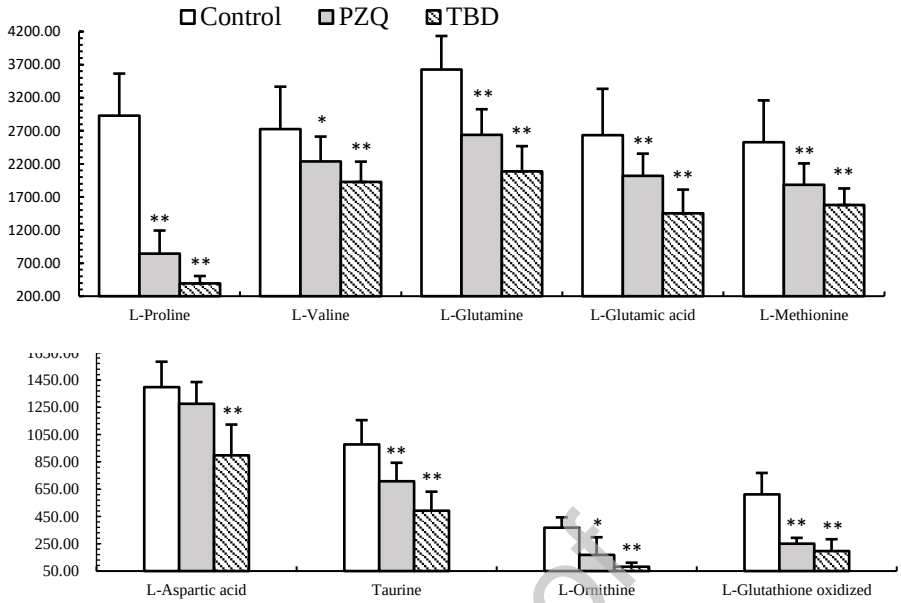

Figure 4. Amino acids (ng/mg) that changed significantly in the TBD group and PZQ group. (*: $p<0.05$, **: $p<0.01$ compared to the control group.)

3.4 Phospholipid metabolism

Phospholipids, an important component of the cell membrane, are essential in the signal transduction and growth regulation of organisms. In our study, 71 phospholipids were detected in *C. sinensis* homogenate samples, of which 17 changed significantly and 10 and 8 apparently increased after treatment with TBD and PZQ, respectively. The representative chromatogram of phospholipids is depicted in Figure 5. The OPLS-DA score plot (Figure 3B) showed the distinct separation of the three groups. As shown in Table 3 and Figure 6, four lysophosphatidyl cholines (LPCs) were highly increased after treatment with TBD, and four LPCs were highly increased after treatment with PZQ. Six lysophosphatidyl ethanolamines (LPEs) were all increased significantly after treatment with TBD. Four sphingomyelins (SM) were decreased, and one phosphatidyl inositol (PI) was increased. The metabolic pathways of the phospholipids are depicted in Figure 7. From the metabolic pathways of Figure

7, it can be seen that LPCs and LPEs are the products of phospholipase A_2 (PLA_2) catalysing the sn-2 acyl of phospholipids. Lysophospholipids are implicated in cell injury, dissolve the cell membrane, and even lead to cell death (Tsujimoto, 2003; Han et al., 2008). In this study, increased LPCs and LPEs may be responsible for the fluke's damaged teguments because of their capability of increasing cell membrane permeability.

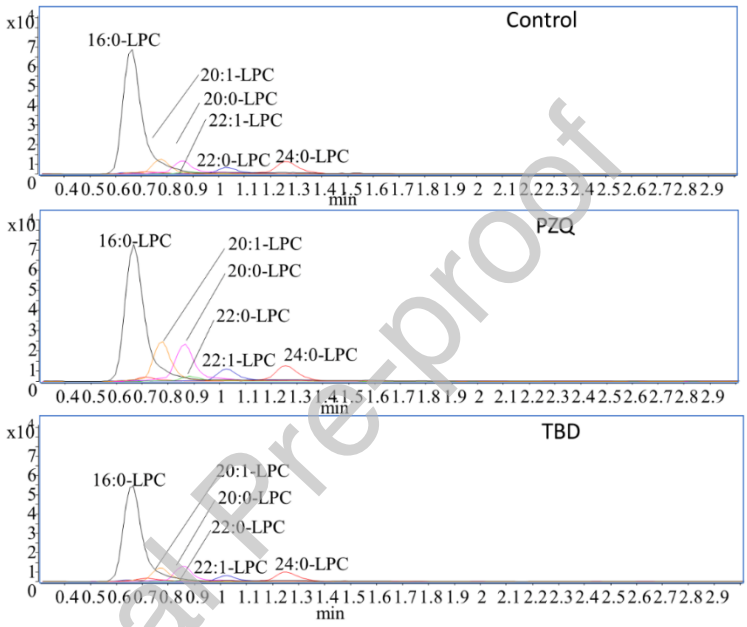

Figure 5. Representative chromatogram of phospholipids in C. sinensis.

Table 3. Significant phospholipids in *C. sinensis* after treatment with PZQ or TBD in rats in vivo.

Metabolites	Control (nmol/g)	PZQ (nmol/g)	TBD (nmol/g)	*p* (Con vs. PZQ)	*p* (Con vs. TBD)	Related pathway
16:0-LPC	298.83±32.96	319.74±67.87	252.48±23.52	-	**	Phosphatidylcholine metabolism
20:1-LPC	35.46±4.79	83.96±35.94	49.68±8.12	*	**	Phosphatidylcholine metabolism
20:0-LPC	36.51±5.38	112.20±60.78	65.03±16.70	*	**	Phosphatidylcholine metabolism
22:1-LPC	4.91±1.10	13.56±6.72	7.36±1.69	*	**	Phosphatidylcholine metabolism
22:0-LPC	19.84±4.12	44.53±21.59	31.00±7.59	*	**	Phosphatidylcholine metabolism
24:0-LPC	34.15±7.58	62.25±30.73	46.84±10.90	-	*	Phosphatidylcholine metabolism
20:2-LPE	25.97±5.12	36.74±16.76	34.38±8.33	-	*	Phosphatidylethanolamine metabolism
20:1-LPE	101.69±25.23	150.25±80.67	153.24±38.37	-	*	Phosphatidylethanolamine metabolism
20:0-LPE	49.92±16.06	81.14±34.70	75.50±20.02	-	*	Phosphatidylethanolamine metabolism
22:2-LPE	12.18±2.79	18.55±10.29	20.15±8.02	-	*	Phosphatidylethanolamine metabolism
22:1-LPE	78.31±22.38	123.66±74.71	126.93±44.49	-	*	Phosphatidylethanolamine metabolism
24:1-LPE	3.74±1.60	6.81±5.08	6.51±2.53	-	*	Phosphatidylethanolamine metabolism

d18:1-20:0-SM	754.39±125.35	812.15±199.11	592.34±66.62	-	*	Sphingomyelin metabolism
d18:0-20:0-SM	814.24±196.06	877.42±226.72	617.48±106.14	-	*	Sphingomyelin metabolism
d18:1-24:1-SM	368.91±65.12	355.65±71.17	267.81±37.30	-	**	Sphingomyelin metabolism
d18:0-24:1-SM	326.97±77.54	344.75±100.17	240.04±51.48	-	*	Sphingomyelin metabolism
18:0/18:0-PI	464.99±138.16	690.28±235.79	633.94±127.78	*	*	Phosphatidyl inositol metabolism

-: $p>0.05$, *: $p<0.05$, **: $p<0.01$.

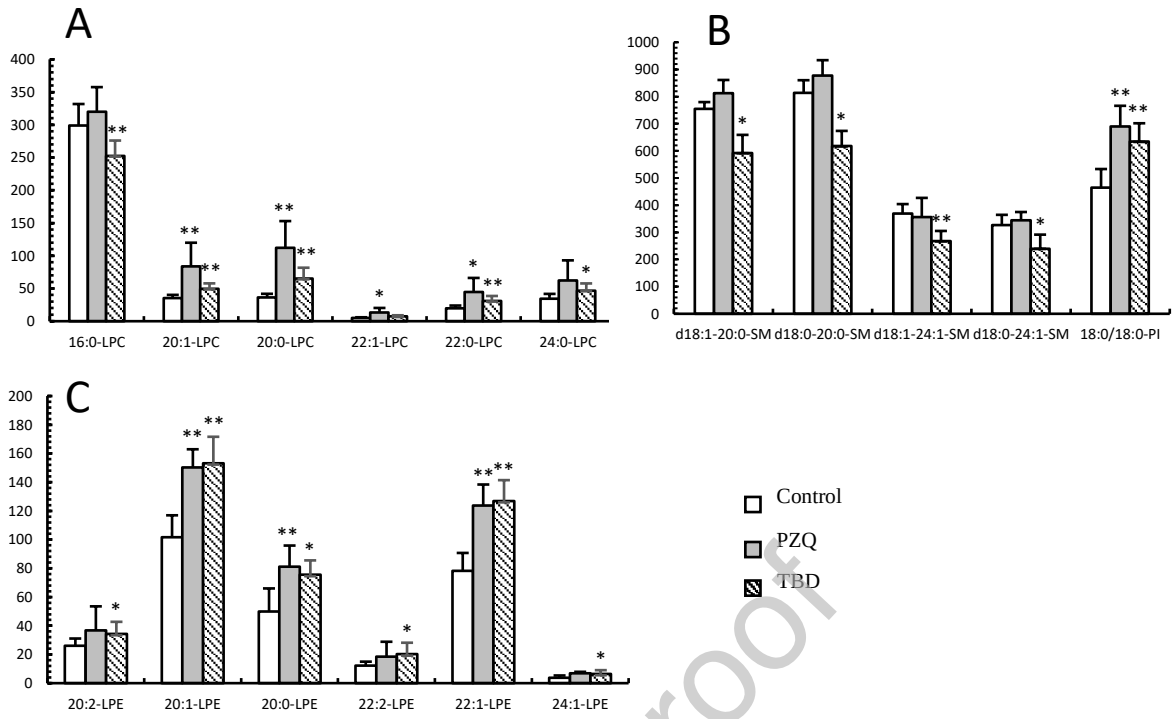

Figure 6. Phospholipids that changed significantly in the TBD group and PZQ group. (A) Six lysophosphatidyl cholines (LPCs). (B) Four sphingomyelins (SM) and one phosphatidyl inositol (PI). (C) Six Lysophosphatidyl ethanolamines (LPE). (*: $p<0.05$, **: $p<0.01$ compared to the control group.)

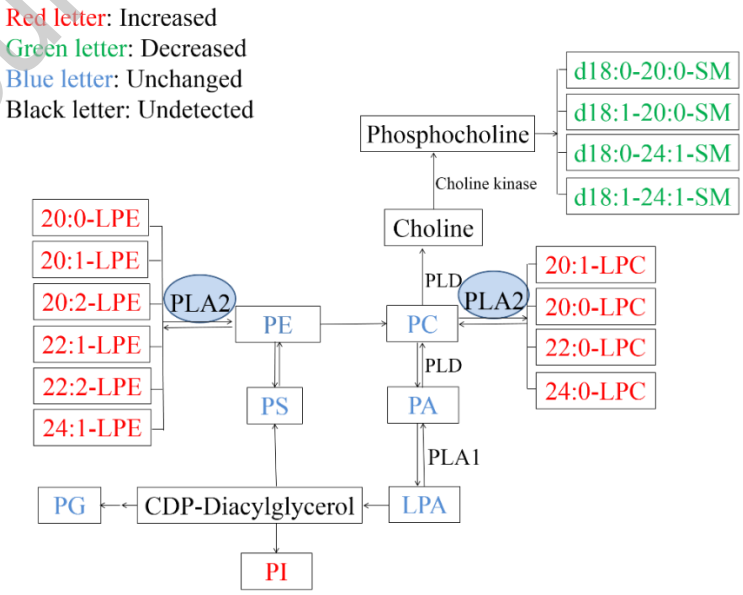

Figure 7. The metabolic pathways of the phospholipids. Significantly increased metabolites after treatment with TBD are coloured red, significantly decreased metabolites are coloured green, metabolites that have no change are coloured blue, and undetected metabolites are coloured black. In the figure, it can be seen that four LPEs and six LPCs increased significantly, and four SMs decreased significantly. Phospholipase A2 hydrolyses PCs to LPCs and hydrolyses PEs to LPEs.

3.5 Fatty acid metabolism

Thirty-seven standards were used to detect the content of fatty acids in *C. sinensis*. Short medium long-chain fatty acids such as C4:0, C6:0, C8:0, C10:0, C11:0 and C12:0 were not detected in *C. sinensis*. This is consistent with the statement that there are mainly higher fatty acids with more than 12 carbons in higher animals and plants (Brondz, 2005). All 27 fatty acids (FAs) detected in C. sinensis were not significantly changed compared with those of the control group. The contents of tall oil fatty acids (ToFAs), saturated fatty acids (SFAs), unsaturated fatty acids (UFAs) and their proportions also did not change significantly.

4 Discussion

Through targeted detection of amino acids, phospholipids and fatty acids in *C. sinensis*, 32 amino acids, 71 phospholipids and 27 fatty acids were detected, of which 10 amino acids and 11 phospholipids had significant changes, but the content of fatty acids had no change.

Amino acids are bioactive molecules in organisms and the basic materials for constructing cells and tissues. Amino metabolites play important roles in the process of biological activities, and their content changes can reflect the different physiological and pathological states of the body to a certain extent (Nilsson et al., 1990; Cuthbertson et al., 2005). Therefore, the detection and analysis of amino

metabolites is of great significance for the diagnosis of related diseases and the study of physiology and pathology. L-proline is metabolized by glutamate in organisms and is the most soluble amino acid in water (Szabados and Savouré, 2010), which may be why it is the most significantly decreased amino acid in this study. Glutamine can regulate the synthesis of protein, stimulate the production of growth hormone, and enhance the immune system. Glutamine deficiency is also closely related to injury to the intestinal intima. Glutamate is the amino acid with the highest abundance in the central nervous system and plays an important role in nerve excitation (Curtis and Watkins, 2010). In this study, L-proline, glutamine and glutamic acid all declined significantly, which may indicate serious degradation of the digestive system, immune system and nervous system as well as energy depletion in *C. sinensis* after treatment with TBD.

Phospholipids are the main biomembrane component. We observed that LPCs and LPEs were significantly increased in *C. sinensis* after treatment with TBD or PZQ. Among the 71 detected phospholipids, four LPCs and six LPEs were apparently increased in the TBD group. Lysophosphatides (including LPCs and LPEs) are the hydrolysate of phospholipase A_2 catalysing the sn-2 acyl of phospholipids (Takahashi et al., 2002; Mcmurray and Magee, 2003), and they can induce various protein kinases, including tyrosine kinases, protein kinase C, and mitogen-activated protein kinases, in vascular endothelial cells (Han et al., 2008). Higher concentrations of endogenous LPC resulted in apoptotic activity. Compared with LPE, LPG, LPI, or LPS, LPC plays more significant roles in lipoapoptosis (Han et al., 2008). Previous papers also showed obvious apoptotic activity of LPC and demonstrated its effect on ruptured red blood cells and other cell membranes, causing haemolysis or cell necrosis (YU and C, 1988; Masamune et al., 2001; Takahashi et al., 2002). The PLA_2/LPC pathways play

important roles in cell death/survival in diverse models of hypoxia, reactive oxygen species damage and reperfusion injury (Williams and Gottlieb, 2002; Cauwels et al., 2003; Tsujimoto, 2003; Yellaturu and Rao, 2003). It is worth noting that after PZQ administration, the surface antigen of flukes is exposed after obvious damage to the tegument, and a large number of eosinophils attach to the surface and invade, causing the worm to die (Harnett and Kusel, 1986; Doenhoff et al., 2008b). In this study, TBD caused rapid and obvious damage to the tegument of *C. sinensis*, resulting in erosion of the tegument and sloughing and exposure of subtegumental tissues. More importantly, after damage to the tegument, the surface antigen was exposed, which made the worm vulnerable to the host's immune attack. Lysophosphatides increased significantly in this study, and electron microscopy results showed that the surfaces of the worms were seriously damaged after treatment with TBD. Therefore, was the damage caused by the effect of TBD on the PLA_2/LPC pathways, which resulted in the significant increase of lysophosphatides that increased the membrane permeability? Was the dual role of the destroyed membrane and the exposed internal antigens the cause of damage and death of *C. sinensis*? Is the PLA2/PLC pathway a target for new drug design? These are questions to be explored in our future research. Based on the smaller doses, rapid onset and fewer side effects compared with PZQ, TBD or the new drugs designed based on the target of TBD may be good substitutes for treating clonorchiasis.

Declaration of Competing Interest

The authors declare that they have no competing interests.

Author statement

Wei Yufen, Liu Xinru and Zhang Haobing conceived of the study, developed the proposal and initiated the writing of the manuscript. Wei Yufen and Liu Xinru were responsible for data analysis and writing of the manuscript. Wei Yufen, Xue Jian and

Huolele were responsible for samples collection and worm burden test. Jiang Zhihua, Chen Yu, Liang Mingyong were responsible for collecting the freshwater fish and identification of metacercariaes. Wei Yufen and Liu Xinru were responsible for sample extraction, LC-MS and GC-MS method development, and metabolites biological analysis.

Acknowledgements

Most heartfelt thanks are given to Jiang Zhihua, Chen Yu and Liang Mingyong for collecting the freshwater fish *Pseudorasbora parva* in the pond of Heng County, Guangxi. This work was supported by the Fifth Round of Three-Year Public Health Action Plan of Shanghai (No. GWV-10.1-XK13).

References:

An, Y., Xu, W., Li, H., Lei, H., Zhang, L., Hao, F., Duan, Y., Yan, X., Zhao, Y., Wu, J., 2013. High-fat diet induces dynamic metabolic alterations in multiple biological matrices of rats. J Proteome Res 12, 3755-3768.

Bligh, E.L.G., Dyer, W.J.A., 1959. A Rapid Method of Total Lipid Extraction and Purification,Can. J. Biochem. Physiol. 37, 911-917. Canadian Journal of Biochemistry & Physiology 37, 911.

Botros, S.S., Bennett, J.L., 2007. Praziquantel resistance. Expert Opin Drug Dis 2, S35.

Boughton, B.A., Callahan, D.L., Silva, C., Bowne, J., Nahid, A., Rupasinghe, T., Tull, D.L., Mcconville, M.J., Bacic, A., Roessner, U., 2011. Comprehensive profiling and quantitation of amine group containing metabolites. Anal Chem 83, 7523-7530.

Brondz, I., 2005. Fatty acids.

Cauwels, A., Janssen, B., Waeytens, A., Cuvelier, C., Brouckaert, P., 2003. Caspase inhibition causes hyperacute tumor necrosis factor-induced shock via oxidative stress and phospholipase A2. Inflamm Res 52, S178-S182.

Ciara, Sullivan, O., Bernard, Fried, Joseph, Sherma, 2013. Metabolic profiling of Echinostoma caproni and Schistosoma mansoni in their definitive and intermediate hosts. Acta Parasitol.

Claus, S.P., Swann, J.R., 2013. Nutrimetabonomics:Applications for Nutritional Sciences, with Specific Reference to Gut Microbial Interactions. Annu Rev Food Sci Technol 4, 381-399.

Coles, G.C., Liang, Y.S., Doenhoff, M.J., 2000. Evidence Against Rapid Emergence

of Praziquantel Resistance in Schistosoma haematobium, Kenya. Emerg Infect Dis 7, 1069-1070.

Curtis, D.R., Watkins, J.C., 2010. THE EXCITATION AND DEPRESSION OF SPINAL NEURONES BY STRUCTURALLY RELATED AMINO ACIDS. J Neurochem 6, 117-141.

Cuthbertson, D., Smith, K., Babraj, J., Leese, G., Waddell, T., Atherton, P., Wackerhage, H., Taylor, P.M., Rennie, M.J., 2005. Anabolic signaling deficits underlie amino acid resistance of wasting, aging muscle. Faseb Journal Official Publication of the Federation of American Societies for Experimental Biology 19, 422-424.

Doenhoff, M.J., Cioli, D., Utzinger, J., 2008a. Praziquantel: mechanisms of action, resistance and new derivatives for schistosomiasis. Curr Opin Infect Dis 21, 659-667.

Doenhoff, M.J., Cioli, D., Utzinger, J., 2008b. Praziquantel: mechanisms of action, resistance and new derivatives for schistosomiasis. Curr Opin Infect Dis 21, 659-667.

Furst, T., Sayasone, S., Odermatt, P., Keiser, J., Utzinger, J., 2012. Manifestation, diagnosis, and management of foodborne trematodiasis. Bmj 344, e4093.

Ghosh, S., Sengupta, A., Sharma, S., Sonawat, H.M., 2012. Metabolic Fingerprints of Serum, Brain, and Liver Are Distinct for Mice with Cerebral and Noncerebral Malaria: A ^{1} H NMR Spectroscopy-Based Metabonomic Study. J Proteome Res 11, 4992-5004.

Gu, L., Jones, A.D., Last, R.L., 2007. LCMS/MS Assay for Protein Amino Acids and Metabolically Related Compounds for Large-Scale Screening of Metabolic Phenotypes. Anal Chem 79, 8067-8075.

Han, M.S., Sun, Y.P., Shinzawa, K., Kim, S., Lee, M.S., 2008. Lysophosphatidylcholine as a death effector in the lipoapoptosis of hepatocytes. J Lipid Res 49, 84.

Harnett, W., Kusel, J.R., 1986. Increased exposure of parasite antigens at the surface of adult male Schistosoma mansoni exposed to praziquantel in vitro. Parasitology 93, 401-405.

Hong, S.T., Fang, Y., 2012. Clonorchis sinensis and clonorchiasis, an update. Parasitol Int 61, 17-24.

Hsu, F.F., Turk, J., 2003. Electrospray ionization/tandem quadrupole mass spectrometric studies on phosphatidylcholines: The fragmentation processes. J Am Soc Mass Spectr 14, 352-363.

Jennifer, K., Jürg, U., 2005. Emerging Foodborne Trematodiasis. Emerg Infect Dis 11, 1507-1514.

Jian, X., Li-Li, X.U., Qiang, H.Q., Zhang, Y.N., Xiao, S.H., 2009. Therapeutic Effect of Tribendimidine,Artesunate and Praziquantel Administered to Hamsters Infected with Clonorchis sinensis. Chinese Journal of Parasitology & Parasitic Diseases.

Keiser, J., Vargas, M., 2010. Effect of artemether, artesunate, OZ78, praziquantel, and tribendimidine alone or in combination chemotherapy on the tegument of Clonorchis sinensis. Parasitol Int 59, 472-476.

Keun, H.C., 2006. Metabonomic modeling of drug toxicity. Pharmacol Therapeut 109, 92-106.

Kim, H., Min, H.K., Kong, G., Moon, M.H., 2009. Quantitative analysis of phosphatidylcholines and phosphatidylethanolamines in urine of patients with breast cancer by nanoflow liquid chromatography/tandem mass spectrometry. Analytical & Bioanalytical Chemistry 393, 1649-1656.

Lal, C.V., Ambalavanan, N., 2015. Biomarkers, Early Diagnosis, and Clinical Predictors of BPD. Clin Perinatol 42, 739-754.

Li, H., An, Y., Zhang, L., Lei, H., Zhang, L., Wang, Y., Tang, H., 2013. Combined NMR and GC-MS analyses revealed dynamic metabolic changes associated with the carrageenan-induced rat pleurisy. J Proteome Res 12, 5520.

Liu, Y.H., Wang, X.G., Gao, P., Qian, M.X., 1991. Experimental and clinical trial of albendazole in the treatment of Clonorchiasis sinensis. Chin Med J 104, 27-31.

Löscher, T., Nothdurft, H.D., Prüfer, L., Sonnenburg, F.V., Lang, W., 1982. Praziquantel in clonorchiasis and opisthorchiasis. Tropenmedizin und Parasitologie 32, 234-236.

Lun, Z., Gasser, R.B., Lai, D., Li, A., Fang, Y., 2005. Clonorchiasis: A key foodborne zoonosis in China. The Lancet Infectious Diseases 5, 31-41.

Masamune, A., Sakai, Y., Satoh, A., Fujita, M., Yoshida, M., Shimosegawa, T., 2001. Lysophosphatidylcholine induces apoptosis in AR42J cells. Pancreas 17, 75-83.

Mcmurray, W.C., Magee, W.L., 2003. Phospholipid Metabolism. Annu Rev Biochem 41, 129-160.

Nicholson, J.K., 2003. 19 Metabonomic approaches to the understanding of direct and idiosyncratic drug toxicity. Toxicol Lett 144, s7-s8.

Nilsson, P., Hillered, L., Pontén, U., Ungerstedt, U., 1990. Changes in cortical extracellular levels of energy-related metabolites and amino acids following concussive brain injury in rats. Journal of Cerebral Blood Flow & Metabolism 10, 631-637.

Prociv, P., 1995. Control of foodborne trematode infections. Report of a WHO Study Group. World Health Organization Technical Report 849, 1.

Qian, M.B., Peiling, Y., Yang, Y.C., Hai, L., Jiang, Z.H., Wei, L., Tan, Y.G., Hui, Z., Jürg, U., Zhou, X.N., 2012. Efficacy and Safety of Tribendimidine Against Clonorchis sinensis. Clinical Infectious Diseases An Official Publication of the Infectious Diseases Society of America, 7.

Qiang, H., 2016. Metabonomic window into hepatitis B virus-related hepatic diseases. World Journal of Hepatology 8, 1.

Ren, H.N., Cheng, B.Z., Zhuang, Z.N., 1987. Experimental therapeutic efficacy of a new anti-hookworm drug, tribendimidin. Chinese Journal of Parasitology & Parasitic Diseases 5, 262-264.

Sonawat, H.M., Sharma, S., 2012. Host Responses in Malaria Disease Evaluated Through Nuclear Magnetic Resonance–Based Metabonomics. Clin Lab Med 32, 129-142.

Szabados, L., Savouré, A., 2010. Proline: a multifunctional amino acid. Trends Plant Sci 15, 97.

Takahashi, M., Okazaki, H., Ogata, Y., Takeuchi, K., Ikeda, U., Shimada, K., 2002. Lysophosphatidylcholine induces apoptosis in human endothelial cells through a p38-mitogen-activated protein kinase-dependent mechanism. Atherosclerosis 161, 387-394.

Tsujimoto, S.Y., 2003. PLA2 activity is required for nuclear shrinkage in caspase-independent cell death. The Journal of Biophysical and Biochemical Cytology 163.

Vennervald, B.J., Polman, K., 2010. Helminths and malignancy. Parasite Immunol 31, 686-696.

Wang, Y., Utzinger, J., Saric, J., Li, J.V., Burckhardt, J., Dirnhofer, S., Nicholson, J.K., Singer, B.H., Brun, R., Holmes, E., 2008. Global metabolic responses of mice to Trypanosoma brucei brucei infection. P Natl Acad Sci Usa 105,

6127-6132.

Wei, Y., Gao, N., Zhang, Z., Zu, X., Hu, Z., Zhang, W., Yin, J., Liu, X., 2016. Metabolic changes at the early stage of sepsis induced by cecal ligation and puncture in rats and the interventional effects of Huang-Lian-Jie-Du-Tang. Journal of Chromatography B.

Williams, S.D., Gottlieb, R.A., 2002. Inhibition of mitochondrial calcium-independent phospholipase A2 (iPLA2) attenuates mitochondrial phospholipid loss and is cardioprotective. Biochem J 362, 23-32.

Xiao, S.H., Jian, X., Tanner, M., Yong-Nian, Z., Keiser, J., Utzinger, J., Hui-Qiang, Q., 2008. Artemether, artesunate, praziquantel and tribendimidine administered singly at different dosages against Clonorchis sinensis: A comparative in vivo study. Acta Trop 106, 54-59.

Xiao, S.H., Jian, X., Tanner, M., Zhang, Y.N., Keiser, J., Utzinger, J., Qiang, H.Q., 2008. Artemether, artesunate, praziquantel and tribendimidine administered singly at different dosages against Clonorchis sinensis: A comparative in vivo study. Acta Trop 106, 54-59.

Xiao, S.H., Wu, H.M., Tanner, M., Utzinger, J., Chong, W., 2005. Tribendimidine: a promising, safe and broad-spectrum anthelmintic agent from China. Acta Trop 94, 1-14.

Xiao, S.H., Xue, J., Xu, L.L., Zheng, Q., Qiang, H.Q., Zhang, Y.N., 2009a. The in vitro and in vivo effect of tribendimidine and its metabolites against Clonorchis sinensis. Parasitol Res 105, 1497-1507.

Xiao, S.H., Xue, J., Xu, L.L., Zheng, Q., Qiang, H.Q., Zhang, Y.N., 2009b. The in vitro and in vivo effect of tribendimidine and its metabolites against Clonorchis sinensis. Parasitol Res 105, 1497.

Xu, Z., Harvey, K., Pavlina, T., Dutot, G., Zaloga, G., Siddiqui, R., 2010. An improved method for determining medium- and long-chain FAMEs using gas chromatography. Lipids 45, 199-208.

Yangco, B.G., Lerma, C.D., Lyman, G.H., Price, D.L., 1987. Clinical study evaluating efficacy of praziquantel in clonorchiasis. Antimicrob Agents Ch 31, 135-138.

Yellaturu, C.R., Rao, G.N., 2003. A Requirement for Calcium-independent Phospholipase A2 in Thrombin-induced Arachidonic Acid Release and Growth in Vascular Smooth Muscle Cells. J Biol Chem 278, 43831-43837.

YU, C, 1988. Cellular ras activity and phospholipid metabolism. Cell 52, 63-71.

Zhao, X., Fritsche, J., Wang, J., Chen, J., Rittig, K., Schmitt-Kopplin, P., Fritsche, A., H Ring, H.U., Schleicher, E.D., Xu, G., 2010. Metabonomic fingerprints of fasting plasma and spot urine reveal human pre-diabetic metabolic traits. Metabolomics 6, 362-374.